Available online at www.sciencedirect.com
ScienceDirect
Journal of Power Sources 160 (2006) 516–522
JOURNAL OF POWER SOURCES
www.elsevier.com/locate/jpowsour

Hydrothermal synthesis of high surface $LiFePO_4$ powders as cathode for Li-ion cells

G. Meligrana [a], C. Gerbaldi [a,*], A. Tuel [b], S. Bodoardo [a], N. Penazzi [a]

[a] *Department of Materials Science and Chemical Engineering, Politecnico di Torino, C.so Duca degli Abruzzi 24, 10129 Turin, Italy*
[b] *Institut de Recherches sur la Catalyse, CNRS (UPR 5401), 2 avenue Albert Einstein, 69626 Villeurbanne Cedex, France*

Received 13 June 2005; received in revised form 19 December 2005; accepted 21 December 2005
Available online 10 February 2006

Abstract

An easy, quick and low cost hydrothermal synthesis was developed to prepare high surface area phospho-olivine $LiFePO_4$ powders to be used as cathode material for Li-ion batteries. The samples were prepared in double distilled water starting from commercial LiOH, $FeSO_4$, H_3PO_4 and using solutions with different concentrations of a surfactant compound (CTAB), in order to increase the specific surface areas, obtaining powders with very small grain size. The structural, morphological and electrochemical properties were investigated by means of X-ray powder diffraction (XRPD), ICP-AES, BET method, scanning electron microscopy (SEM) and constant current charge–discharge cycling. The electrochemical performances of $LiFePO_4$ prepared in this manner showed to be positively affected by the presence of CTAB during synthesis, showing capacities near the theoretical value, only slightly affected by the discharge regime (from *C*/20 to 10*C*).

Keywords: Lithium-ion cell; Lithium iron phosphate; Cathode material; Hydrothermal synthesis; Surfactant; Galvanostatic cycling test

1. Introduction

It is well known that the main efforts in the development of Li-ion systems regard the portable electronic devices, like portable phones, camcorders and lap-top computers, trying to increase the battery power density, and the huge market of electric vehicles (EVs) and hybrid-electric vehicles (HEVs) where low cost, low pollution but high specific performance batteries are needed [1,2]. In particular, the investigation into new materials for the positive electrode is one of the basic lines of research.

Since the pioneering works of Padhi et al. [3], mixed orthophosphates $LiMPO_4$ (where M = Mn, Fe, Co, Ni) isostructural to olivine have been intensively studied as lithium insertion cathode materials for the next generation of Li-ion secondary batteries [4]. Among these compounds, the mineral triphylite, having the formula $LiFePO_4$ and showing an ordered olivine structure, has proved to be one of the most promising among the polyanionic compounds tested over recent years [3,5].

This compound shows several advantages compared with conventional cathode materials such as $LiCoO_2$, $LiNiO_2$ and $LiMnO_2$, namely it is lower in toxicity and relatively inexpensive. In addition, $LiFePO_4$ has an interesting theoretical specific capacity of about 170 mAh g^{-1}, a good cycle stability and a technically attractive flat voltage versus current profile of 3.45 V versus Li^+/Li, due to the two-phase extraction/insertion mechanism. A further advantage of this material, thanks to its stability, is the improved safety at high temperatures compared to the transition-metal oxides that lose oxygen on overcharging, which increases the probability of electrolyte decomposition at higher temperatures.

Lithium iron phosphate, at the first charge, can de-intercalate 1 Li^+ ion per formula unit, corresponding to the oxidation of Fe^{2+} to Fe^{3+}. The extraction of Li^+ ions gives rise to a new phase, $FePO_4$ (heterosite), which maintains nearly the same structure: *a* and *b* lattice constants decrease slightly while *c* increases [2,3]. This feature assures that the process is highly reversible and repeatable.

The first investigations on $LiFePO_4$ as electrode material have put in evidence that the capacity reached at room temperature is far below the theoretical one. Moreover, a reversible capacity loss is present throughout the charge–discharge cycles,

* Corresponding author. Tel.: +39 011 5644638; fax: +39 011 5644699.
E-mail address: claudio.gerbaldi@polito.it (C. Gerbaldi).

0378-7753/$ – see front matter © 2006 Elsevier B.V. All rights reserved.
doi:10.1016/j.jpowsour.2005.12.067

increasing with the current density [3,5]. This capacity loss seems to be related to the limited area of the interface between the $LiFePO_4/FePO_4$ phases where the Li^+ extraction/insertion takes place. According to Andersson and Thomas, the factor limiting the full conversion of $LiFePO_4$ to $FePO_4$ is based on the combination of low lithium ion diffusion rate and poor electronic conductivity [6].

It has been readily recognized that the grain size is a critical issue to minimize high current capacity loss; e.g. Yamada et al. obtained 95% of theoretical capacity at room temperature and at current density higher than 0.1 mA cm^{-2} using samples having 20 μm particle size [5].

Apart from increasing temperature, which can have a positive influence but is impractical for Li-ion batteries directed to a wide market, another possible way of improving $LiFePO_4$ performance has been followed by Ravet et al. [7,8], who succeeded in coating the grains with carbon, so improving the capacity through an increase of conductivity. The same method was undertaken by many researchers using organic materials, like sucrose, added during preparation [9,10]. Our research group, in particular, carried out investigations on phospho-olivine compounds using ascorbic acid and citric acid as carbonaceous additives [2,11]. Prosini et al. obtained interesting results by adding fine particles of carbon black during the synthesis [12]. Croce et al. improved the kinetic properties of $LiFePO_4$ by dispersing copper or silver into the solution during synthesis [13]. The finely dispersed metal powder promoted a reduction of particle size and an increase in the material conductivity. It was also claimed that the electronic conductivity of $LiFePO_4$ could be increased by doping with metals supervalent to Li^+ (i.e. Mg^{2+}, Al^{3+}) [14].

The next logical step was to try to get an efficient charge transport preparing a homogeneous active material with refined grains size and intimate carbon contact. Huang et al. [15] obtained higher current density capacities from a $LiFePO_4$/C composite containing 15% of carbon and a 100–200 nm particle size. In a review article, illustrating the progress in the design of olivine-type cathodes at Sony, Yamada et al. [16] showed a cathode material preparation involving an addition of a "disordered conductive carbon" added to the precursor of the material, being 3% the minimum amount, and a subsequent stage of high energy ball milling to get nano-scale homogenized particles.

Experience in this field has clearly shown that carbonaceous materials added to the precursors during synthesis have a fundamental importance in increasing the $LiFePO_4$ performance. They can act as reducing agents to avoid the formation of trivalent Fe ions during firing, maintain the particles isolated from each other preventing their coalescence and enhance intra and inter particle conductivity. The choice of the additive is, therefore, of marked importance: it will exert the deep influence previously described only if it can take part in the process itself, like in the synthetic routes followed by Huang et al. [15].

In this context, the kind of synthesis used becomes important too. Initially, the most common way of synthesizing $LiFePO_4$ was the solid-state route [5,17], that we also followed in our first investigations [2,11]. Nevertheless, we obtained higher performing $LiMPO_4$ (where M = Fe, Mn) materials via a sol–gel synthetic route [18]. The amorphous precursors used allowed the production of sub-micrometric agglomerates smaller than those prepared via solid-state route and produced a very homogeneous carbon dispersion in the phosphate phase. More recently, hydrothermal preparation has been preferentially chosen for its advantages: quick, easy to perform, low cost in energy and easily scalable. Yang et al. [10] obtained 3 μm $LiFePO_4$ particles, smaller than the 20 μm $LiFePO_4$ grains obtained by Yamada et al. [5] with a solid-state reaction.

Our recent investigations, of which the first results are reported in the present paper, concern the hydrothermal synthesis of $LiFePO_4$ powders using an organic surfactant compound (hexadecyltrimethylammonium bromide, hereafter reported as CTAB), which is added during synthesis. Our aim was to investigate the influence of this additive on the preparation of the materials. As a dispersing agent it probably modifies the structure of the crystallites more deeply than just decrease their grain size. Moreover, with the firing of the synthesized samples in inert atmosphere, the CTAB remaining after the filtering stage gives rise to a carbon coating that increases the conductivity of the materials and enhances their electrochemical performance.

2. Experimental

2.1. Synthesis

The lithium iron phosphate samples were prepared by direct mild hydrothermal synthesis. Starting materials were $FeSO_4{\cdot}7H_2O$ (Aldrich, purity 99%), H_3PO_4 (Aldrich, purity >85%), LiOH (Aldrich, purity >98%) in the stoichiometric ratio 1:1:3 and hexadecyltrimethylammonium bromide (Aldrich, $C_{19}H_{42}BrN$, CTAB). First of all, a CTAB water solution was prepared, stirring the white powder in distilled water at 35 °C for approximately 30 min in order to completely dissolve it. $FeSO_4$ and H_3PO_4 water solutions were prepared and mixed together. The resulting solution was then added to the surfactant solution under constant stirring and only in the end, so avoiding the formation of $Fe(OH)_2$ which can be easily oxidized to Fe^{3+}, LiOH was added. The mixture, whose pH ranged between 7.2 and 7.5, was vigorously stirred for 1 min and then quickly transferred in a Teflon-lined stainless steel autoclave and heated at 120 °C for 5 h. The autoclave was then cooled to room temperature and the resulting green precipitate washed, via a standard procedure to ensure complete elimination of the excess of surfactant, filtered and dried at 40 °C overnight. The heating treatment was carried out in inert atmosphere to avoid the oxidation of Fe^{2+} to Fe^{3+}: the powders were pre-treated at 200 °C (heating rate of 5.0 °C min^{-1}) and then fired at 600 °C (2.0 °C min^{-1}) in pure N_2 for 12 h in order to obtain the crystalline phase and to carbonise the surfactant, so obtaining a carbon film that homogeneously covers the grains.

The four samples obtained in this manner are hereafter named LF1 (sample obtained without CTAB addition during synthesis), LF2 (4.11 mmol CTAB added during synthesis), LF3 (6.87 mmol CTAB) and LF4 (13.70 mmol CTAB).

2.2. Chemical, structural analysis and surface area determination

Quantitative elemental analysis was carried out by inductively coupled plasma-atomic emission spectroscopy (ICP-AES) with a Varian Liberty 100 instrument. The samples were digested in hot concentrated $HCl:HNO_3 = 3:1$ mixture. The weight percentage of carbon in the samples was determined by a C, H, N Analyzer model 1106 Carlo Erba Strumentazione.

The X-ray diffraction profiles of the samples were obtained using a Philips Xpert MPD powder diffractometer, equipped with Cu Kα radiation ($V = 40$ kV, $i = 30$ mA) and a curved graphite secondary monochromator. The diffraction data were collected in the 2θ-range between 15 and 80°, with an acquisition step of 0.02° and a time per step of 10 s.

The samples were also submitted to a scanning electron microscope (SEM) investigation for morphological characterization, using a Hitachi S800 microscope (INSA, Lyon) with a magnification of 6×10^4.

Specific surface areas (SSA) were determined using the Brunauer, Emmet, Teller (BET) method on an ASAP 2010 Micromeritics instrument. Prior to adsorption, approximately 50.0 mg of solid was placed in the cell and evacuated at 350 °C for 5 h.

2.3. Cathode and cell preparation, electrochemical tests

The electrodes for the evaluation of the electrochemical properties were prepared spreading on an aluminum current-collector, by the so-called "doctor blade" technique, a slurry of the $LiFePO_4$ active material (70 wt%) with carbon black as electronic conductor (Super P, MMM Carbon Belgium) (20 wt%) and poly(vinylidene fluoride) as binder (PVdF, Solvay Solef 6020) (10 wt%) in *N*-methyl-2-pyrrolidone (NMP, Aldrich). After the evaporation of the solvent by a mild heating, disks of 0.785 cm^2 were punched out of the foil and dried by heating them at about 130 °C under high vacuum for 5 h. After their transfer in an Ar-filled dry glove box, the disks were weighed before their use in the test cells and, by subtraction of the average weight of the Al disks, the weight of the coating mixture was calculated. The composite electrodes were used in three electrode T-cells with lithium metal as anode and a glass-wool (Whatman GF/A) disc as the separator. The liquid electrolyte used was 1 M $LiPF_6$ in a 1:1 mixture of ethylene carbonate (EC) and diethyl carbonate (DEC) (Merck).

The galvanostatic cycling tests were carried out at room temperature with an Arbin Instrument Testing System model BT-2000, setting the cut off voltages to 2.50–4.00 V versus Li^+/Li. The charge–discharge cycles were set at the same rate ranging from *C*/20 to 10*C*.

3. Results and discussion

3.1. Chemical and structural characterization

Elemental analysis results gave the basic characterization of the synthesized materials. The results, reported in Table 1, show that for all the samples prepared using CTAB during synthesis, the expected $LiFePO_4$ stoichiometry was obtained. The molar ratio for Li:Fe:P is almost 1:1:1 for the three samples prepared in the presence of CTAB; major divergences are observed in the case of sample LF1. As for carbon, it is interesting to observe that the content is, for LF4, markedly superior to the other samples.

Table 1
Elemental composition of the materials (expressed in wt% of total weight)

Sample	CTAB (mmol)	Li (wt%)	Fe (wt%)	P (wt%)	C (wt%)
LF1	0.0	3.5	35.4	14.6	–
LF2	4.11	3.7	33.5	15.6	1.11
LF3	6.87	3.8	33.1	15.8	1.52
LF4	13.70	4.1	33.9	17.8	4.80

Fig. 1 shows the X-ray powder diffraction patterns of the samples synthesized in the presence of the surfactant. The purity degree is high: the main diffraction peaks can be attributed to the orthorhombic $LiFePO_4$ olivine-type phase. Some minor peaks are due to impurities, which can be mainly attributed to $Li_3Fe_2(PO_4)_3$, α-Fe and hematite Fe_2O_3. The sample LF4, in particular, looks very pure and its narrow diffraction peaks indicate a good crystallinity degree. The sample LF1, prepared without CTAB addition, is not reported in the figure as the X-ray powder diffraction data put in evidence a material constituted by a mixture of various ferrous and ferric phosphates, like $Fe_3(PO_4)_3{\cdot}8H_2O$, $Li_3Fe_2(PO_4)_3$, Fe_2O_3 and only a little amount of $LiFePO_4$, a result somehow expected from the divergences in the molar ratio. Therefore, this sample cannot be compared with the others, which are prepared in presence of CTAB.

As all the samples prepared in the presence of the surfactant were submitted to a firing stage at 600 °C (2.0 °C min^{-1}) in pure N_2, the presence of a carbonaceous phase, due to the decomposition of the organic species, still present after washing and filtering, has to be expected. Nevertheless, there is no evidence of such phase in the diffraction patterns, probably because

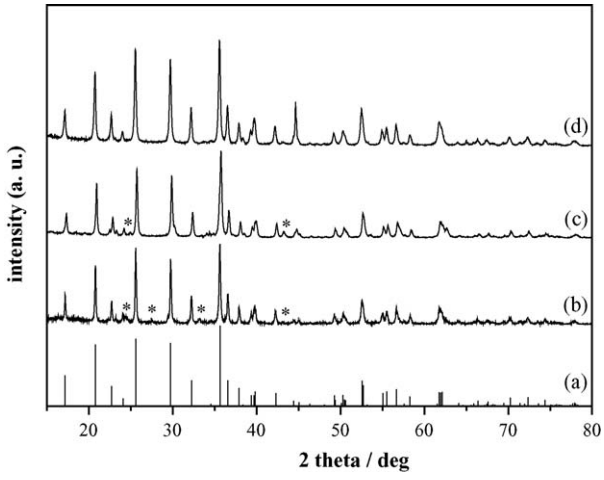

Fig. 1. X-ray powder diffraction patterns of the $LiFePO_4$ samples, synthesized under hydrothermal conditions using different concentrations of the organic surfactant (CTAB) and calcined under flowing N_2 at 600 °C for 12 h. (a) Theoretical $LiFePO_4$, (b) LF2, (c) LF3 and (d) LF4. The asterisks indicate the reflection peaks of the impurity phases.

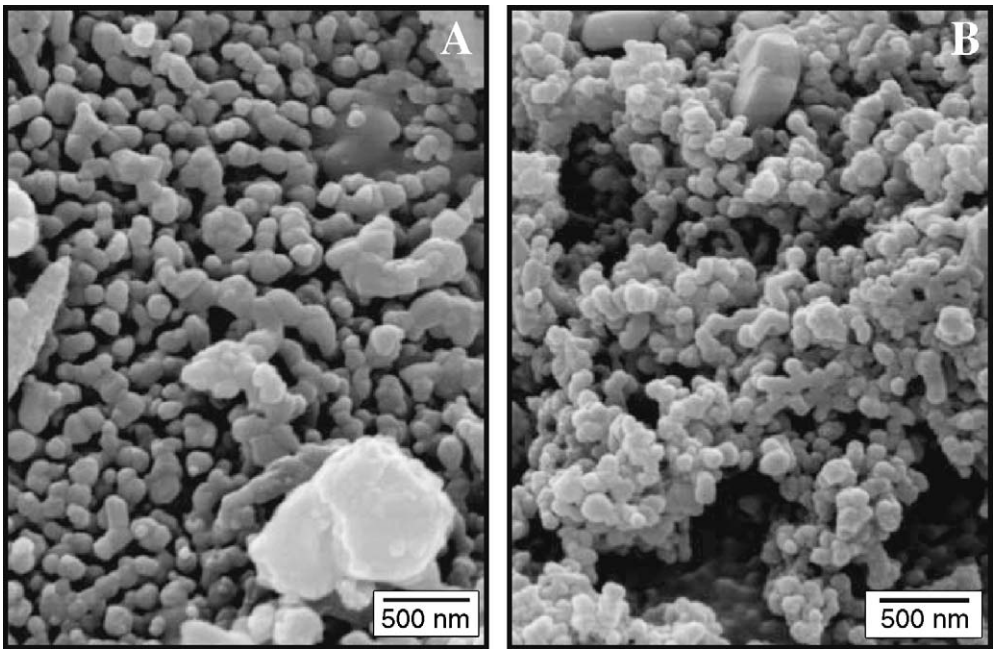

Fig. 2. Scanning electron micrographs of the LF2 (A) and LF4 (B) samples, both annealed at 600 °C in inert atmosphere.

it is present in a low content and/or it is amorphous, causing only a little increase of the background in the low-angle region.

The SEM microphotographs, reported in Fig. 2A and B, put in evidence the strong grain-refining effect of CTAB, which is directly related to its amount. The sample LF2 shows grain dimensions of about 90–100 nm (Fig. 2A), while the size of the LF4 grains is estimated around 50 nm, see Fig. 2B. In the same figure, the particles seem also more homogeneous in size with less signs of coalescence between the grains to form boulders like in Fig. 2A. This effect of refining and homogenizing the size of the grains induced by the presence of an organic species has been already reported [5,15,16]. Our experience states that, in this respect, CTAB appears one of the most effective additive tested [2,11,18].

A confirmation, quite valuable being quantitative, of the positive influence of the surfactant on the grain characteristics comes from specific surface area measurements with the BET method. The data reported in Table 2 show that CTAB markedly enhances the specific surface area of the powders. The sample LF2 shows a specific surface area almost three times more extended than the sample prepared without CTAB. Also important is the fact that this increase is dependent on the amount of CTAB; in fact, the data indicate an almost linear dependence of SSA versus mmol of CTAB in the synthesis solution. Unfortunately, due to solubility limitations, it is difficult to investigate the effect of the presence of CTAB in higher amounts.

Table 2
Specific surface area (SSA, $m^2\,g^{-1}$) related to the molar amount of CTAB (mmol) used in the synthesis of the different samples

Sample	SSA ($m^2\,g^{-1}$)	CTAB (mmol)
LF1	4.27	0
LF2	11.60	4.11
LF3	26.80	6.87
LF4	44.70	13.70

3.2. Electrochemical measurements

The electrochemical performance of the materials, tested in a laboratory cell versus a lithium metal anode, are shown in Figs. 3 and 4. The figures report the galvanostatic discharge profiles of the samples at *C*/20 (Fig. 3) and *C*/5 (Fig. 4) extracted from cycling tests carried out at increasing *C*-rates. The results for the sample LF1 are not reported in these figures as they cannot be compared to the others, being LF1 constituted by different phases. The curves put in evidence the superior performance of LF4 sample, which, in addition, shows a more definite discharge

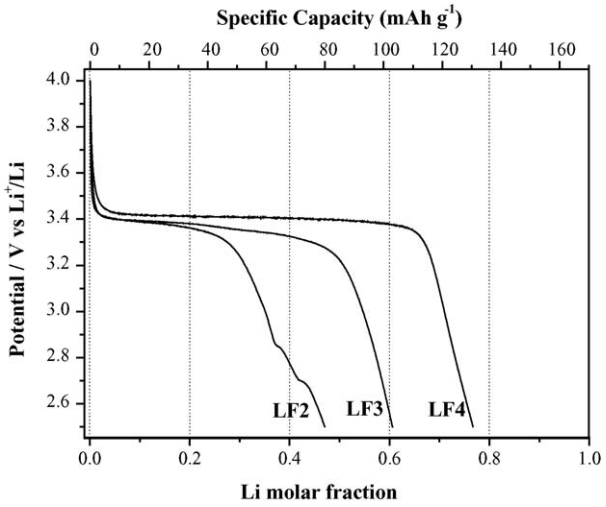

Fig. 3. Discharge profiles vs. lithium at *C*/20 for the $LiFePO_4$ samples (3rd cycle of the cycling test, 3rd cycle at *C*/20). Current density = 8.5 mAh g^{-1}.

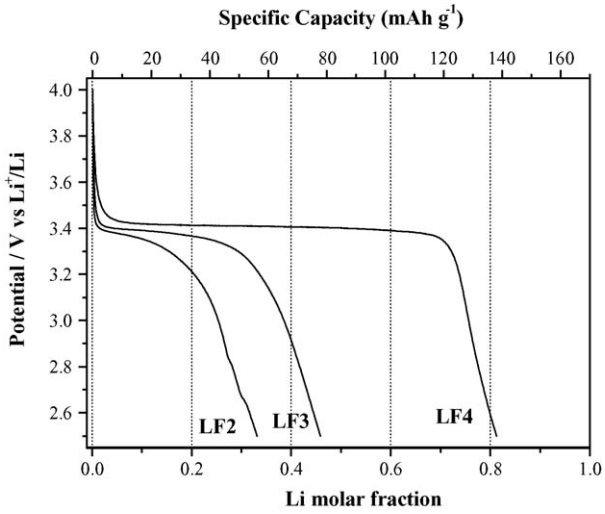

Fig. 4. Discharge profiles vs. lithium at *C*/5 for the $LiFePO_4$ samples (18th cycle of the cycling test, 3rd cycle at *C*/5). Current density = 34 mAh g^{-1}.

step with a steep potential decay at its end. A second point of interest is the similar specific capacity value shown by the sample LF4 at the two discharge regimes chosen, suggesting the apparent independence from the discharge rate. Unfortunately, this is not completely true: this feature depends from the particular ongoing of the first cycles of sample LF4, as it will be discussed in the following figures.

The specific capacity of the samples at higher current regimes and their cyclability are interesting too. Fig. 5 shows the cycling behaviour of the samples LF2, LF3 and LF4 at room temperature, at charge–discharge regimes ranging from *C*/20 to 1*C*. In general, all the curves show a good cycling stability at a certain regime, the charge coefficient (charge capacity/following discharge capacity) being very near to one. The results of the most recent durability tests with hundreds of cycles, confirm this statement. A feature peculiar only to sample LF4 is the progressive lowering of the charge capacity at the initial cycles, while the discharge capacity correspondingly increases. This low performance at the beginning explains the similar value of specific capacity detected in Fig. 4 with respect to Fig. 3. Such unbalanced situation soon stabilizes giving values of the charge coefficient near 1. This initial behaviour, not so evident in the other samples, seems to be tied to the initial cycling phase; it has the appearance of an "induction" period during which the material stabilizes its behaviour.

The progressive increase of the discharge capacity is not a new feature. Similar phenomena have been reported by several authors [4,12,15,22,23], some of which did not try an explanation whatsoever. Zhang et al. [23], considered $LiFePO_4$ samples prepared with a carbon content of 3–10 wt%, all showing this increase in capacity during initial cycling. Such initial irreversibility, has been related, at least partially, to a "self doping of Li^+ ions into Fe sites". At the moment, lacking any clarifying experimental finding, we can only relate the phenomenon to the high amount of carbon present in the sample LF4. We suppose that the extended carbon layer which covers the grains allows the complete migration of Li^+ ions outside the material causing structural modifications inside the grains and at the interface between $LiFePO_4$ and carbon layer. The situation is progressively restored during what have been called the induction cycles. A deeper insight of this topic can be achieved by getting additional structure information (e.g. from Raman spectra and Rietveld refining of X-ray powder diffraction patterns).

The plot of Fig. 6 reports the results of another cycling test on sample LF4, at room temperature, extended to 10*C*. Apart from the confirmation of the very good performance, the plot puts in evidence the good cycling stability of this sample, which shows a high rate capability and even a slight progressive improvement of the charge coefficient at higher discharge regimes. The performance is at the level of the best results of the literature [4,15,17,19–21] and ours [2,11,18], particularly at higher discharge regimes, which is very important.

The plot of Fig. 7 summarizes the performance of the studied materials with respect to the discharge rate until 10*C*, at which regime the sample LF4 still maintains the 65% of the theoretical capacity. The initial upward going of the LF4 curve for *C*/20 and *C*/10 cycling rates is a consequence of the anomalous behaviour of the first cycles for this samples (see Fig. 5). So *C*/20 and

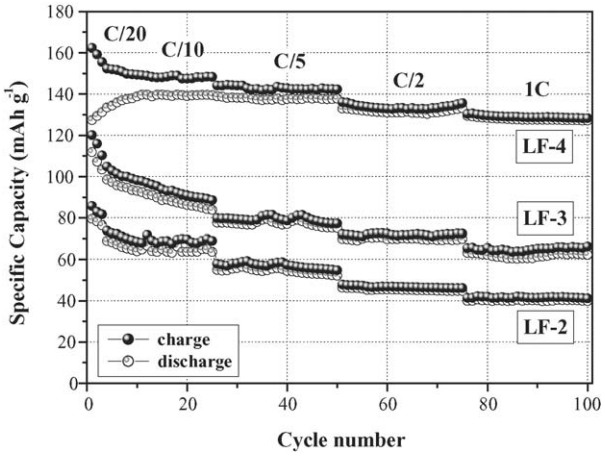

Fig. 5. Cycling performance of LF2, LF3 and LF4 samples at *C*-rates from *C*/20 to 1*C*.

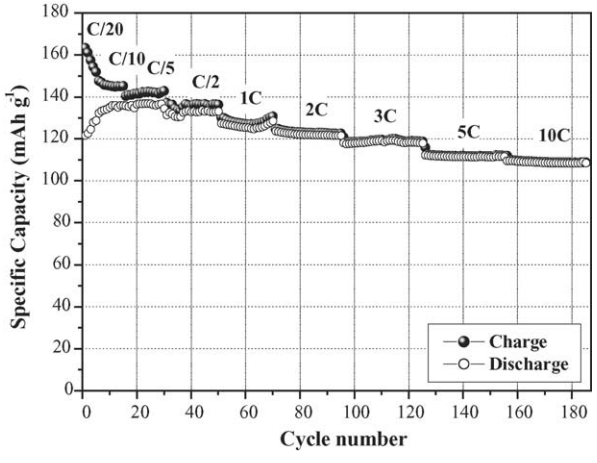

Fig. 6. Charge–discharge cycling test of LF4 at different *C*-rate (from *C*/20 to 10*C*).

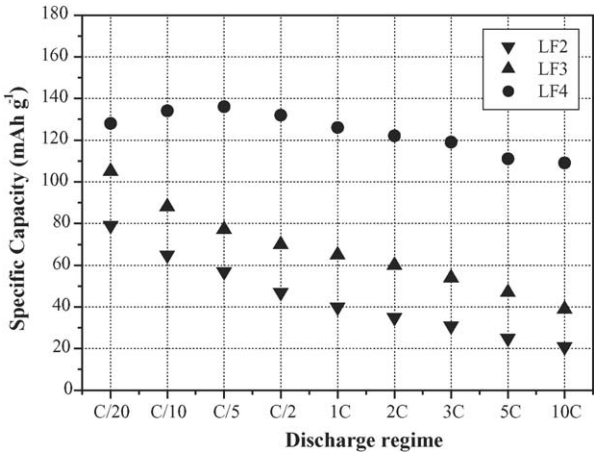

Fig. 7. Specific capacity of the samples at different *C*-rate (from *C*/20 to 10*C*). Each value is the average among the capacity values of the cycles at the corresponding rate.

C/10, whose data come actually from the curve of Fig. 6, show, in Fig. 7, a value of the specific capacity lower than *C*/5. Another specific feature of the sample LF4 is that the capacity loss with the increasing of the current is quite limited. From *C*/10 to 10*C* the capacity of LF4 shows a lowering of about 15%, while for LF2 and LF3 the value is doubled.

The experimental results presented allow to state that CTAB influences the electrochemical properties of $LiFePO_4$ in several ways. Its action is exerted both during the very preparation of the material and in the following firing stage. During synthesis, the CTAB micelles limit the growth of large crystallites, possibly by segregating the crystalline seeds, favouring their dispersion and homogenizing their size. This leads to an increase of the SSA and it makes the electrolyte accessible to a more extended region of the active material. Then, during the firing stage at 600 °C in inert atmosphere, the surfactant exerts, as a carbonaceous material, a reducing action preventing Fe^{2+} from being oxidized to Fe^{3+}, so ensuring the purity of the samples. More important, the carbon layer produced as a consequence of the firing of the organic species, deposits on the grains surface and it acts as an electronic conductor enhancing at a nanoscopic level the transfer of electrons. Moreover, as the volume occupied by the organic surfactant is lowered when carbon is obtained, voids could be formed between the particles, favouring the access of the electrolyte and the passing of Li^+ ions to and from the material.

The sum of these phenomena allow to realize the optimum conditions for $LiFePO_4$ action as cathode material for lithium ion batteries. The role played by carbon is still to be put in evidence experimentally: our first HR-TEM observations of the samples (not reported here) seem to confirm our point of view.

4. Conclusions

An easy, quick and low cost hydrothermal synthesis in the presence of an organic surfactant compound (CTAB) allowed to prepare $LiFePO_4$ powders with outstanding features as cathode material for Li-ion cells.

The results obtained in this work have shown that the presence of CTAB is essential to obtain the desired material; moreover, when it is added in high amounts, the cycling performance and the discharge capacity of the samples are markedly enhanced and present typical features.

CTAB leads to the preparation of powders with finely dispersed nanocrystalline grains of pure material, also acting on the degree of agglomeration of the grains and hence on the extent of the specific surface area. The pyrolysis of CTAB during the firing step produces a strongly reductive atmosphere that prevents the oxidation of Fe^{2+} to Fe^{3+} ensuring the purity of the synthesis product, and improves the conductivity of the material with the in situ coated carbon film on the $LiFePO_4$ particles.

The results presented in this paper have shown that the LF4 sample, prepared in presence of the highest amount of CTAB, shows an electrochemical performance comparable to the best literature results.

Acknowledgements

The Italian Government (PRIN 2002032512_006 funding) contributed in financing the present research. The help of Prof. B. Scrosati of the University of Rome "La Sapienza" in forwarding technical instrumentation is gratefully acknowledged. Thanks are also due to Dr. M. Malandrino of the University of Turin for the ICP-AES analysis.

References

[1] B. Scrosati, Nature 373 (1995) 557.
[2] M. Piana, M. Arrabito, S. Bodoardo, A. D'Epifanio, D. Satolli, F. Croce, B. Scrosati, Ionics 8 (2002) 17.
[3] A.K. Padhi, K.S. Nanjundaswamy, J.B. Goodenough, J. Electrochem. Soc. 144 (1997) 1188.
[4] S. Franger, F. Le Cras, C. Bourbon, H. Rouault, J. Power Sources 119–121 (2003) 252.
[5] A. Yamada, S.C. Chung, K. Hinokuma, J. Electrochem. Soc. 148 (2001) A224.
[6] A.S. Andersson, J.O. Thomas, J. Power Sources 97–98 (2001) 498.
[7] N. Ravet, J.B. Goodenough, S. Besner, M. Simoneau, P. Hovington, M. Armand, in: Proceedings of the ECS Meeting, Abstracts 99-2 (1999) 127.
[8] N. Ravet, Y. Chouinard, J.F. Magnan, S. Besner, M. Gauthier, M. Armand, Abstract of IMLB-10 (2000) 166.
[9] N. Ravet, Y. Chouinard, J.F. Magnan, S. Besner, M. Gauthier, M. Armand, J. Power Sources 97–98 (2001) 503.
[10] S. Yang, P.Y. Zavalij, M.S. Whittingham, Electrochem. Commun. 3 (2001) 505.
[11] N. Penazzi, M. Arrabito, M. Piana, S. Bodoardo, S. Panero, I. Amadei, J. Eur. Ceram. Soc. 24 (2004) 1381.
[12] P.P. Prosini, D. Zane, M. Pasquali, Electrochim. Acta 46 (2001) 3517.
[13] F. Croce, A. D'Epifanio, J. Hassoun, A. Deptula, T. Olczac, B. Scrosati, Electrochem. Solid State Lett. 5 (3) (2002) A47.
[14] S. Chung, J.T. Bloking, Y. Chiang, Nat. Mater. 1 (2002) 123.
[15] H. Huang, S.-C. Yin, L.F. Nazar, Electrochem. Solid State Lett. 4 (10) (2001) A170.
[16] A. Yamada, M. Hosoya, S.-C. Chung, Y. Kudo, K. Hinokuma, K.-Y. Liu, Y. Nishi, J. Power Sources 119–121 (2003) 232.
[17] A.S. Andersson, J.O. Thomas, B. Kalska, L. Häggström, Electrochem. Solid State Lett. 3 (2) (2000) 66.

[18] M. Piana, B.L. Cushing, J.B. Goodenough, N. Penazzi, Solid State Ionics 175 (2004) 233.
[19] S. Yang, Y. Song, P.Y. Zavalij, M.S. Whittingham, Electrochem. Commun. 4 (2002) 239.
[20] Z. Chen, J.R. Dahn, J. Electrochem. Soc. 149 (9) (2002) A1184.
[21] P. Reale, S. Panero, B. Scrosati, J. Garche, M. Wohlfahrt-Mehrens, M. Wachtler, J. Electrochem. Soc. 151 (12) (2004) A2138.
[22] T.-H. Cho, H.-T. Chung, J. Power Sources 133 (2004) 272.
[23] S.S. Zhang, J.L. Allen, K. Xu, T.R. Jow, J. Power Sources 147 (2005) 234.